

## N O T I C E

THIS DOCUMENT HAS BEEN REPRODUCED FROM  
MICROFICHE. ALTHOUGH IT IS RECOGNIZED THAT  
CERTAIN PORTIONS ARE ILLEGIBLE, IT IS BEING RELEASED  
IN THE INTEREST OF MAKING AVAILABLE AS MUCH  
INFORMATION AS POSSIBLE

NASA Technical Memorandum 87140



## Carbon Films Grown from Plasma on III-V Semiconductors

(NASA-TM-87140) CARBON FILMS GROWN FROM  
PLASMA ON III-V SEMICONDUCTORS (NASA) 12 p  
HC A/2/MF AJ1 CSCL 09C

N86-12135

Unclas  
G3/76 27674

J.J. Pouch, J.D. Warner,  
and D.C. Liu  
*Lewis Research Center  
Cleveland, Ohio*

Prepared for the  
One hundred and sixty-eighth Meeting of the Electrochemical Society  
Las Vegas, Nevada, October 11-17, 1985

**NASA**

## CARBON FILMS GROWN FROM PLASMA ON III-V SEMICONDUCTORS

J.J. Pouch, J.D. Warner, and D.C. Liu  
National Aeronautics and Space Administration  
Lewis Research Center  
Cleveland, Ohio 44135

### ABSTRACT

Dielectric carbon films were grown on n- and p-type GaAs and InP substrates using plasmas generated at 30 KHz from gaseous hydrocarbons. The effect of gas source, flow rate, and power on film growth were investigated. Methane and n-butane gases were utilized. The flow rate and power ranged from 30 to 50 sccm and 25 to 300 W, respectively.

AES measurements show only carbon to be present in the films. The relative Ar ion sputtering rate (3 KeV) of carbon depends on the ratio power/pressure. In addition, the degree of asymmetry associated with the carbon-semiconductor interface is approximately power-independent. SIMS spectra indicate different H-C bonding configurations to be present in the films. Band gaps as high as 3.05 eV are obtained from optical absorption studies.

### Introduction

Carbon films exhibiting unique properties can be formed on different substrates by ion-beam deposition (1), ion-beam sputtering (2,3,5,6) and plasma decomposition of gaseous hydrocarbons (4-7). These films are generally hard and semi-transparent. The electrical resistivity can be greater than  $10^{13} \Omega\text{-cm}^8$ . The films may be useful as optical coatings. In addition, they may impact process areas in the semiconductor technology, e.g., metal-insulator-metal (MIM) fabrication (9), and device encapsulation and passivation.

There is presently an increasing need to grow dielectric films on III-V semiconductors for metal-insulator-semiconductor field-effect transistor (MISFET) applications (10). The dielectric must be a high quality insulator, and the deposition process must not introduce a high interface state density which would degrade the device performance.

In this investigation, carbon films were grown on GaAs and InP substrates by means of plasma chemical vapor deposition (CVD) at 30 KHz. The influence of growth conditions on film properties were studied by Auger electron spectroscopy (AES), x-ray photoelectron spectroscopy (XPS), secondary ion mass spectrometry (SIMS) and UV/VIS/NIR spectrophotometry. Breakdown fields were obtained from

electrical measurements performed on metal-insulator-semiconductor (MIS) structures (carbon was used as the insulator).

### Experimental

A planar plasma reactor operating at 30 KHz was utilized for the carbon depositions. The power was capacitively coupled to the upper electrode, and the bottom electrode and chamber wall were grounded. The chamber pressure was controlled by the input gas flow rate and pumping speed. The gas sources were  $\text{CH}_4$  and  $\text{C}_4\text{H}_{10}$ . The substrates were  $\langle 100 \rangle$  GaAs and InP crystals grown by the liquid encapsulated Czochralski (LEC) method. Dopant concentrations were  $\sim 10^{17} \text{ cm}^{-3}$ ; room temperature mobilities were  $\sim 2700 \text{ cm}^2/(\text{V}\cdot\text{sec})$ . After standard cleaning (4), the samples were placed on the grounded anode inside the chamber. The background pressure was  $\sim 20 \text{ mTorr}$ . The deposition gas ( $\text{CH}_4$  or  $\text{C}_4\text{H}_{10}$ ) was used to flush the system three times prior to each run. Amorphous carbon films were produced by subjecting the substrates to the ac glow discharge. The power and flow rate settings covered the ranges 25 to 300 W and 30 to 90 sccm, respectively. The initial substrate temperature was  $25^\circ\text{C}$ , and it increased a few degrees during each deposition.

In order to study the electrical properties of the MIS structures, an ohmic contact was made to the rear surface of a n-type GaAs wafer by thermal evaporation of Au-Ge, Ni, and Au. Annealing was performed in a  $\text{N}_2$  ambient at  $425^\circ\text{C}$  for 5 min, followed by thermal evaporation of Al onto the carbon film surface.

### Results and Discussions

Auger depth profiles of the films were obtained using a PHI AES/XPS/SIMS system interfaced with a multiple technique analytical computer system (MACS). Sputtering was done with 3 KeV Ar ions at 25 mA. The sensitivity of the AES measurements indicated that the films contained only carbon in the bulk, and a few percent of oxygen at the film-semiconductor interface. These results were independent of the source gas used for the depositions. A representative AES profile of a carbon film deposited from  $\text{C}_4\text{H}_{10}$  on InP is shown in Fig. 1. The flow rate is 30 sccm (corresponding to a steady-state pressure of 175 mTorr), and the power is 25 W.

The relative Ar ion sputtering rate,  $G$ , at fixed power, is defined by the relation  $G = t_p/t_d$ , where  $t_p$  is the AES profiling time for the carbon film and  $t_d$  is the deposition time (11). Figure 2 shows the dependence of  $G$  (for 3 KeV Ar ions) on the ratio power/pressure (proportional to average energy per particle) for two  $\text{C}_4\text{H}_{10}$  pressures: 175 and 245 mTorr. We note that  $G$  becomes sensitive to the chamber pressure for power/pressure ratios  $\geq 0.85$ .

The degree of asymmetry associated with the carbon-semiconductor interface is proportional to  $\delta = Bx(T_R - 2T_M + T_L)$  where B is a constant, and  $T_R$ ,  $T_M$ , and  $T_L$  are the AES sputtering times corresponding to the carbon peak-to-peak signals at 10, 50, and 90 percent of the maximum attained in a depth profile, respectively. The influence of  $\text{CH}_4$  flow rate on  $\delta$  is presented in Fig. 3 for several powers. The results indicate that  $\delta$  is approximately power-independent in the 50 to 300 W range (fixed pressure). It appears that  $\delta$  (fixed power) approaches zero (symmetric interface) as the chamber pressure is increased.

A 10 KeV Al  $K_{\alpha}$  x-ray source was used for XPS studies. The deposition gas was  $\text{CH}_4$  and the power varied from 25 to 300 W. It was determined that the asymmetry in the C 1s lineshape decreased with power for a total chamber pressure of 245 mTorr. This trend is presumably influenced by the amount of hydrogen contained in the films.

Relative counts of hydrocarbon ions sputtered from carbon (substrate-InP) were determined from SIMS depth profiling studies (performed with 3 KeV Ar ions). In Fig. 4(a), the distribution of ion counts is plotted as a function of mass-to-charge ratio for various deposition conditions ( $\text{C}_4\text{H}_{10}$  plasma). The predominant ion is  $(\text{CH})^+$ , and contributions from  $(\text{CH}_2)^+$ ,  $(\text{CH}_3)^+$ ,  $(\text{C}_2\text{H})^+$ ,  $(\text{C}_2\text{H}_2)^+$ , and  $(\text{C}_2\text{H}_3)^+$  are evident.

Figure 4(b) shows the ion distribution obtained from carbon films prepared by a methane discharge. We note that  $(\text{CH})^+$  has a higher probability of being sputtered from each film. (In comparison, Figs. 4(a) and (b) indicate that the lowest populations are associated with  $(\text{CH}_3)^+$ .) These results depict some of the H-C bonding arrangements which are prevalent in the plasma-deposited films (12).

A SIMS depth profile (3 KeV Ar ions) of carbon deposited on GaAs is presented in Fig. 5. Mass windows for  $\text{Ga}^+$ ,  $\text{As}^+$ ,  $\text{O}^+$ , and  $\text{CH}_x^+$  ( $x = 0,1,2,3$ ) were utilized. The  $\text{CH}_x^+$  distributions are uniform in the bulk of the film, and they drop to lower levels in the substrate region. In addition, Fig. 5 shows oxygen to be present throughout the carbon film. (This determination was not possible with the less-sensitive AES technique.) Finally, it is apparent that  $\text{Ga}^+$  and  $\text{As}^+$  are readily detected as the carbon film is sputtered.

Figure 6 shows a SIMS depth profile of carbon on InP.  $\text{In}^+$ ,  $\text{P}^+$ ,  $\text{O}^+$ , and  $\text{CH}_x^+$  ( $x = 0,1,2,3$ ) were monitored. The  $\text{CH}_x^+$  ( $x = 0,1,2$ ) distributions are uniform in the film region, and progressively lower levels are attained in the vicinity of the film-InP interface. We note that the  $\text{O}^+$  and  $\text{CH}_3^+$  profiles are "noisy." Figure 6 illustrates that  $\text{In}^+$  and  $\text{P}^+$  concentrations are being detected during the film sputtering process.

Measurements of optical absorption as a function of photon energy for carbon films deposited on fused silica plates were made with a UV/VIS/NIR spectrophotometer (Perkin-Elmer, model Lambda 9). Prior to the film measurements, the sample compartment was continuously purged with dry N<sub>2</sub>, and a scan of the background for data correction was made over the photon energy range. A slit width of 2 nm was used for the film measurements. In addition, a blank fused silica plate was placed in the reference beam path. The differences in film and silica plate reflectivities were not taken into account.

Figure 7 illustrates the dependence of  $(AE)^{1/2}$  as a function of  $E$  for a carbon film deposited on the silica plate. The absorbance is  $A$  and the photon energy is  $E$ . (The C<sub>4</sub>H<sub>10</sub> flow rate and power were 50 sccm and 150 W, respectively.) In order to determine the optical band gap,  $E_g$ , we referred to a theoretical model describing interband optical absorption in a noncrystalline solid (13). We estimate  $E_g \sim 3.05$  eV. In comparison, we note that  $E_g$  for carbon films on InP obtained from plasma decomposition of CH<sub>4</sub> is typically  $<2.35$  eV (11).

Capacitance-voltage measurements (1 MHz) of the MIS structures on GaAs yielded a flat C-V curve. This results suggests Fermi level pinning of the carbon-GaAs interface. The phenomenon is probably attributable to the existence of a large interface state density.

Breakdown fields (V/cm) and dielectric constants are summarized in Table I for various deposition conditions. The power was fixed at 100 W. The breakdown strength of the carbon films can therefore be enhanced by substituting C<sub>4</sub>H<sub>10</sub> for CH<sub>4</sub> in the deposition process. In addition, we note that the dielectric constants for as-prepared films are in the range 2.5 to 4.3.

### Conclusions

We have demonstrated that carbon films can be deposited on GaAs and InP by means of plasma decomposition of gaseous hydrocarbons (CH<sub>4</sub> and C<sub>4</sub>H<sub>10</sub>). AES measurements show only carbon to be present in the films. The relative Ar ion sputtering rate (3 KeV) of carbon depends on the ratio power/pressure. In addition, the degree of asymmetry associated with the carbon-semiconductor interface is approximately power-independent. SIMS spectra indicate different H-C bonding configurations to be present in the films. Band gaps as high as 3.05 eV are obtained from optical absorption studies.

### Acknowledgment

We thank Dr. Samuel Alterovitz for reviewing this manuscript and for stimulating discussions.

#### REFERENCES

1. S. Aisenberg and R. Chabot, J. Appl. Phys. 42, 2953 (71).
2. B.A. Banks and S.K. Rutledge, J. Vac. Sci. Technol. 21, 807 (82).
3. A.A. Khan, J.A. Woollam, Y. Chung, and B.A. Banks, IEEE Elect. Dev. Letts. EDL-4, 146 (83).
4. J.D. Warner, J.J. Pouch, S.A. Alterovitz, D.C. Liu, and W.A. Lanford, J. Vac. Sci. Technol. A3, 900 (85).
5. C.W. Weissmantel, G. Reisse, H.J. Erler, F. Henny, K. Bewilogua, U. Ebersback, and C. Shurer, Thin Solid Films 63, 315 (79).
6. D. Mathine, R.O. Dillon, A.A. Khan, G. Bu-Abbud, J.A. Woollam, D.C. Liu, B.A. Banks, and S. Domitz, J. Vac. Sci. Technol. A2, 365 (84).
7. R.O. Dillon, J.A. Woollam, and V. Katkanant, Phys. Rev. B29, 3482 (84).
8. K. Fuzii, N. Shohata, M. Mikami, and M. Yonezawa, Appl. Phys. Lett. 47, 370 (85).
9. J. Lamb and J.A. Woollam, J. Appl. Phys. 57, 5420 (85).
10. D.C. Liu, G.J. Valco, G.G. Skebe, and V.J. Kapoor, Electrochem. Soc. Proc. 83-8, 161 (83).
11. J.J. Pouch, S.A. Alterovitz, J.D. Warner, D.C. Liu, and W.A. Lanford, Mat. Res. Soc. Symp. Proc. San Francisco, CA, April, 1985 (accepted for publication).
12. A. Benninghoven, Surf. Sci. 53, 596 (75).
13. N.F. Mott and E.A. Davis, Electronic Processes in Noncrystalline Materials (Clarendon Press, Oxford) 291 (79).

TABLE I. - DIELECTRIC CONSTANTS AND  
 BREAKDOWN FIELDS FOR CARBON FILMS  
 DEPOSITED ON n-GaAs

Deposition parameters	Dielectric constant	Breakdown field, V/cm
CH <sub>4</sub> , 100 W 30 sccm	3.4	1.8x10 <sup>6</sup>
CH <sub>4</sub> , 100 W 50 sccm	4.3	6.5x10 <sup>5</sup>
C <sub>4</sub> H <sub>10</sub> , 100 W 30 sccm	3.2	6.0x10 <sup>6</sup>
C <sub>4</sub> H <sub>10</sub> , 100 W 50 sccm	2.5	5.6x10 <sup>6</sup>



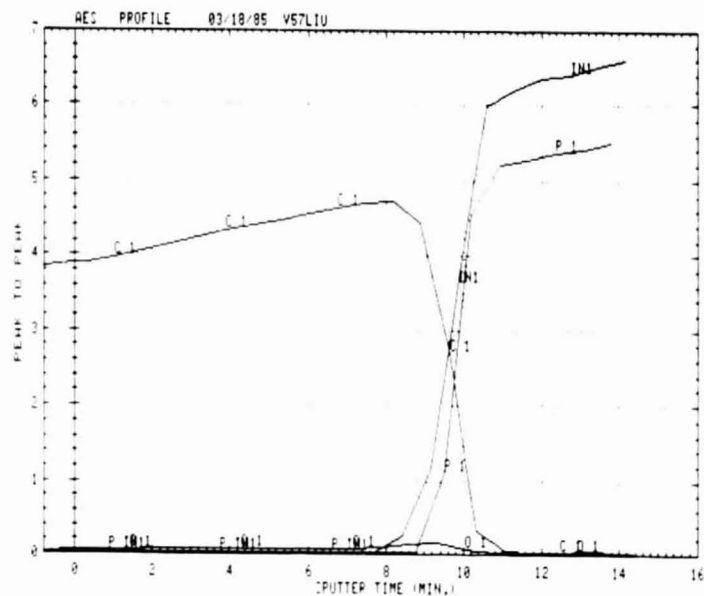


Figure 1. - AES depth profile of carbon on InP. Deposition parameters:  
 $C_4H_{10}$ , 30 sccm, 25 W.

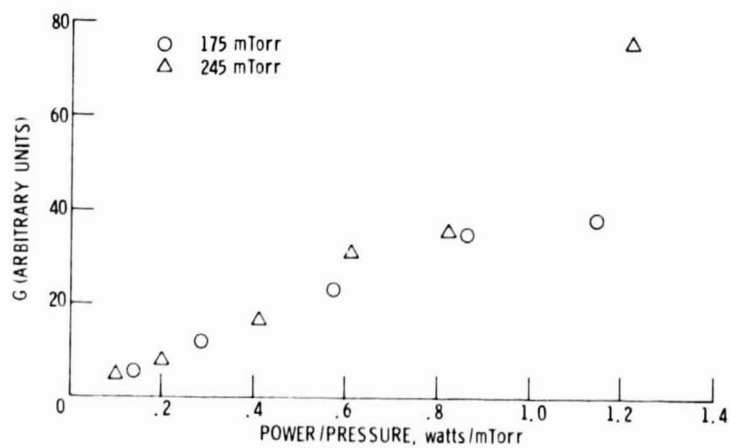


Figure 2. - Relative Ar ion sputtering rate as a function of the ratio power / pressure for carbon on InP.

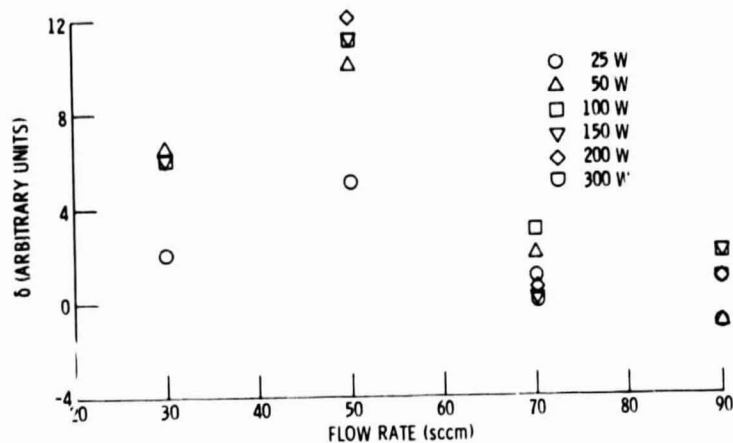


Figure 3. -  $\delta$  versus  $\text{CH}_4$  flow rate for carbon on InP.

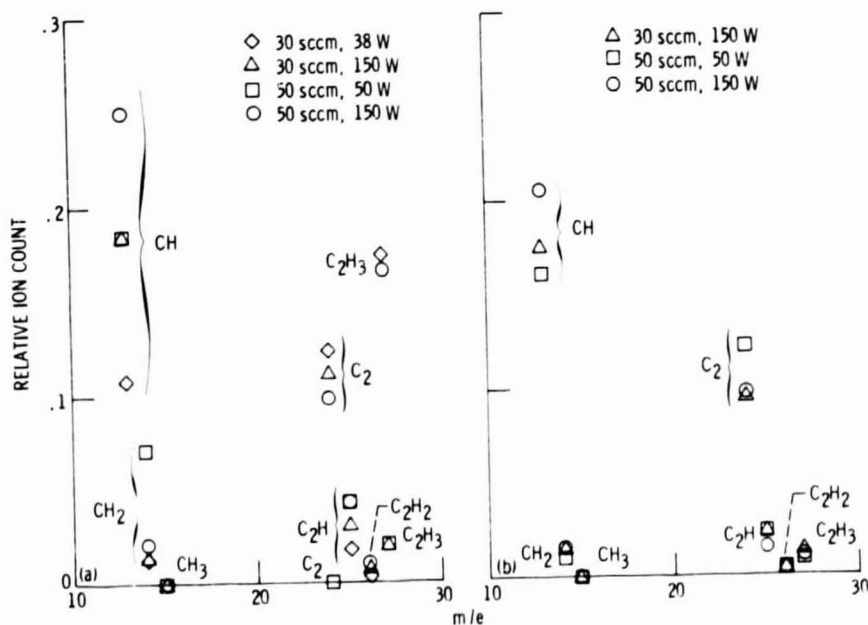


Figure 4. - Relative ion count as a function of mass-to-charge ratio for carbon deposited on InP using  $\text{C}_4\text{H}_{10}$  (a) and  $\text{CH}_4$  plasmas (b).

ORIGINAL FACE IS  
OF POOR QUALITY

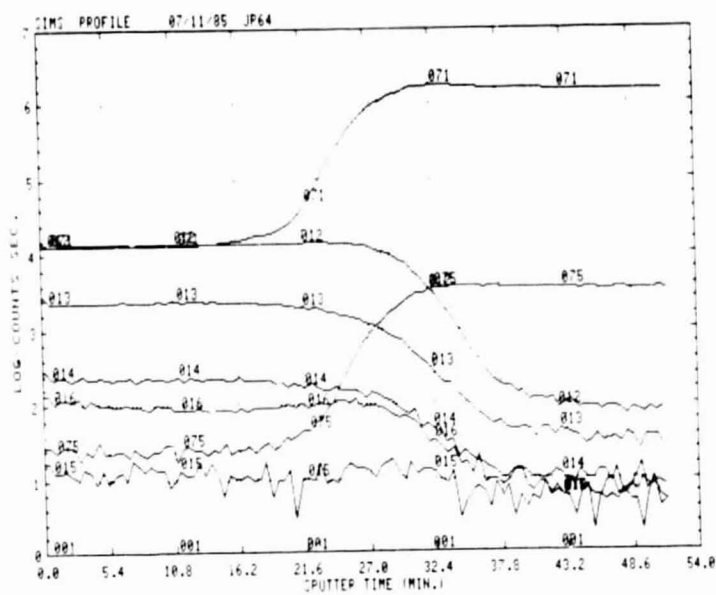


Figure 5. - SIMS depth profile of carbon on GaAs.

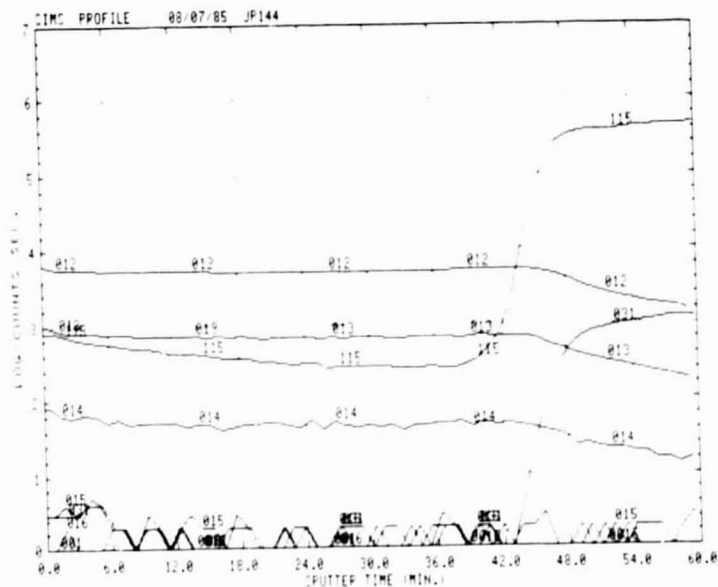


Figure 6. - SIMS depth profile of carbon on InP.

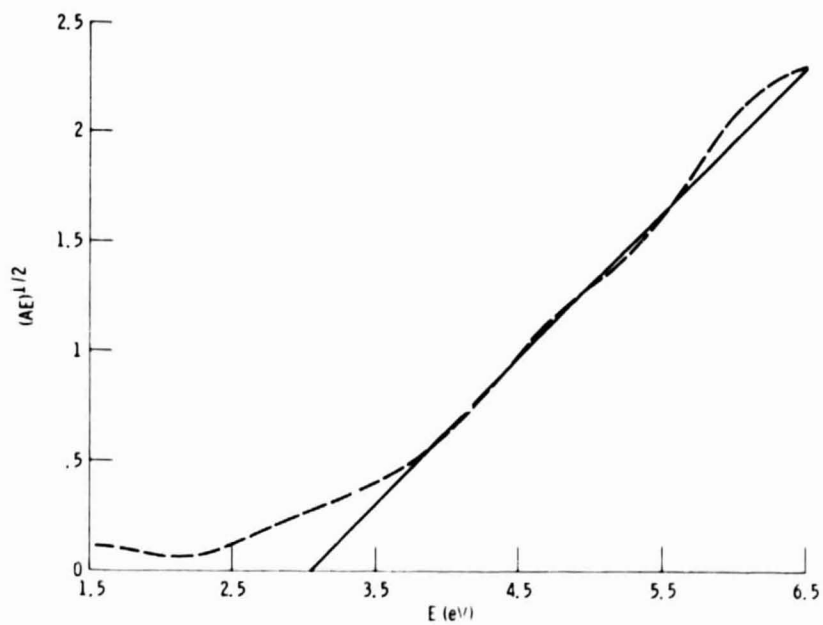


Figure 7.  $-(AE)^{1/2}$  versus  $E$  for carbon on fused silica. The straight line is a least squares fit to the data. Deposition parameters:  $C_4H_{10}$ , 50 sccm, 150 W.